

Study of $J/\psi \rightarrow p\bar{p}, \Lambda\bar{\Lambda}$ and observation of $\eta_c \rightarrow \Lambda\bar{\Lambda}$ at Belle

C.-H. Wu,²² M.-Z. Wang,²² K. Abe,⁶ I. Adachi,⁶ H. Aihara,⁴⁰ V. Aulchenko,¹
 T. Aushev,¹⁰ S. Bahinipati,⁴ A. M. Bakich,³⁶ V. Balagura,¹⁰ A. Bay,¹⁵ K. Belous,⁹
 U. Bitenc,¹¹ I. Bizjak,¹¹ S. Blyth,²⁰ A. Bondar,¹ A. Bozek,²³ T. E. Browder,⁵ Y. Chao,²²
 A. Chen,²⁰ W. T. Chen,²⁰ B. G. Cheon,³ Y. Choi,³⁵ Y. K. Choi,³⁵ A. Chuvikov,³¹
 S. Cole,³⁶ J. Dalseno,¹⁷ M. Danilov,¹⁰ M. Dash,⁴⁴ S. Eidelman,¹ N. Gabyshev,¹
 T. Gershon,⁶ A. Go,²⁰ G. Gokhroo,³⁷ A. Gorišek,¹¹ H. Ha,¹³ J. Haba,⁶ K. Hayasaka,¹⁸
 H. Hayashii,¹⁹ M. Hazumi,⁶ D. Heffernan,²⁸ T. Hokuue,¹⁸ S. Hou,²⁰ W.-S. Hou,²²
 Y. B. Hsiung,²² T. Iijima,¹⁸ K. Inami,¹⁸ A. Ishikawa,⁴⁰ R. Itoh,⁶ M. Iwasaki,⁴⁰ Y. Iwasaki,⁶
 J. H. Kang,⁴⁵ S. U. Kataoka,¹⁹ N. Katayama,⁶ H. Kawai,² T. Kawasaki,²⁵ H. R. Khan,⁴¹
 H. Kichimi,⁶ H. J. Kim,¹⁴ H. O. Kim,³⁵ Y. J. Kim,⁶ P. Križan,^{16, 11} P. Krokovny,⁶
 R. Kulasiri,⁴ R. Kumar,²⁹ C. C. Kuo,²⁰ A. Kuzmin,¹ Y.-J. Kwon,⁴⁵ G. Leder,⁸ J. Lee,³⁴
 Y.-J. Lee,²² T. Lesiak,²³ S.-W. Lin,²² D. Liventsev,¹⁰ G. Majumder,³⁷ F. Mandl,⁸
 T. Matsumoto,⁴² A. Matyja,²³ S. McOnie,³⁶ W. Mitaroff,⁸ K. Miyabayashi,¹⁹
 H. Miyake,²⁸ H. Miyata,²⁵ Y. Miyazaki,¹⁸ R. Mizuk,¹⁰ T. Mori,⁴¹ E. Nakano,²⁷
 M. Nakao,⁶ Z. Natkaniec,²³ S. Nishida,⁶ O. Nitoh,⁴³ S. Ogawa,³⁸ T. Ohshima,¹⁸
 T. Okabe,¹⁸ S. Okuno,¹² S. L. Olsen,⁵ Y. Onuki,²⁵ H. Ozaki,⁶ P. Pakhlov,¹⁰ H. Palka,²³
 H. Park,¹⁴ K. S. Park,³⁵ R. Pestotnik,¹¹ L. E. Pilonen,⁴⁴ Y. Sakai,⁶ T. Schietinger,¹⁵
 O. Schneider,¹⁵ A. J. Schwartz,⁴ R. Seidl,^{7, 32} M. E. Sevier,¹⁷ M. Shapkin,⁹ H. Shibuya,³⁸
 V. Sidorov,¹ A. Sokolov,⁹ A. Somov,⁴ N. Soni,²⁹ S. Stanič,²⁶ M. Starič,¹¹ H. Stoeck,³⁶
 T. Sumiyoshi,⁴² F. Takasaki,⁶ M. Tanaka,⁶ G. N. Taylor,¹⁷ Y. Teramoto,²⁷ X. C. Tian,³⁰
 T. Tsuboyama,⁶ T. Tsukamoto,⁶ S. Uehara,⁶ T. Uglov,¹⁰ K. Ueno,²² S. Uno,⁶ P. Urquijo,¹⁷
 Y. Usov,¹ G. Varner,⁵ C. C. Wang,²² C. H. Wang,²¹ Y. Watanabe,⁴¹ E. Won,¹³
 B. D. Yabsley,³⁶ A. Yamaguchi,³⁹ Y. Yamashita,²⁴ L. M. Zhang,³³ and Z. P. Zhang³³

(The Belle Collaboration)

¹*Budker Institute of Nuclear Physics, Novosibirsk*

²*Chiba University, Chiba*

³*Chonnam National University, Kwangju*

⁴*University of Cincinnati, Cincinnati, Ohio 45221*

⁵*University of Hawaii, Honolulu, Hawaii 96822*

⁶*High Energy Accelerator Research Organization (KEK), Tsukuba*

⁷*University of Illinois at Urbana-Champaign, Urbana, Illinois 61801*

⁸*Institute of High Energy Physics, Vienna*

⁹*Institute of High Energy Physics, Protvino*

¹⁰*Institute for Theoretical and Experimental Physics, Moscow*

¹¹*J. Stefan Institute, Ljubljana*

¹²*Kanagawa University, Yokohama*

¹³*Korea University, Seoul*

¹⁴*Kyungpook National University, Taegu*

¹⁵*Swiss Federal Institute of Technology of Lausanne, EPFL, Lausanne*

¹⁶*University of Ljubljana, Ljubljana*

- ¹⁷*University of Melbourne, Victoria*
¹⁸*Nagoya University, Nagoya*
¹⁹*Nara Women's University, Nara*
²⁰*National Central University, Chung-li*
²¹*National United University, Miao Li*
²²*Department of Physics, National Taiwan University, Taipei*
²³*H. Niewodniczanski Institute of Nuclear Physics, Krakow*
²⁴*Nippon Dental University, Niigata*
²⁵*Niigata University, Niigata*
²⁶*University of Nova Gorica, Nova Gorica*
²⁷*Osaka City University, Osaka*
²⁸*Osaka University, Osaka*
²⁹*Panjab University, Chandigarh*
³⁰*Peking University, Beijing*
³¹*Princeton University, Princeton, New Jersey 08544*
³²*RIKEN BNL Research Center, Upton, New York 11973*
³³*University of Science and Technology of China, Hefei*
³⁴*Seoul National University, Seoul*
³⁵*Sungkyunkwan University, Suwon*
³⁶*University of Sydney, Sydney NSW*
³⁷*Tata Institute of Fundamental Research, Bombay*
³⁸*Toho University, Funabashi*
³⁹*Tohoku University, Sendai*
⁴⁰*Department of Physics, University of Tokyo, Tokyo*
⁴¹*Tokyo Institute of Technology, Tokyo*
⁴²*Tokyo Metropolitan University, Tokyo*
⁴³*Tokyo University of Agriculture and Technology, Tokyo*
⁴⁴*Virginia Polytechnic Institute and State University, Blacksburg, Virginia 24061*
⁴⁵*Yonsei University, Seoul*

Abstract

We study the baryonic charmonium decays of B mesons, $B^+ \rightarrow \eta_c K^+$ and $B^+ \rightarrow J/\psi K^+$, where the η_c and J/ψ subsequently decay into a $p\bar{p}$ or $\Lambda\bar{\Lambda}$ pair. We measure the $J/\psi \rightarrow p\bar{p}$ and $\Lambda\bar{\Lambda}$ anisotropy parameters, $\alpha_B = -0.60 \pm 0.13 \pm 0.14$ ($p\bar{p}$), $-0.44 \pm 0.51 \pm 0.31$ ($\Lambda\bar{\Lambda}$) and compare to results from $e^+e^- \rightarrow J/\psi$ formation experiments. We also report the first observation of $\eta_c \rightarrow \Lambda\bar{\Lambda}$. The measured branching fraction is $\mathcal{B}(\eta_c \rightarrow \Lambda\bar{\Lambda}) = (0.87_{-0.21}^{+0.24}(stat)_{-0.14}^{+0.09}(syst) \pm 0.27(\text{PDG})) \times 10^{-3}$. This study is based on a 357 fb^{-1} data sample recorded on the $\Upsilon(4S)$ resonance with the Belle detector at the KEKB asymmetric-energy e^+e^- collider.

PACS numbers: 13.25.Gv, 14.40.Gx, 13.40.Hq

There have been many observations of baryonic three-body B decays in recent years [1, 2, 3, 4, 5]. An interesting feature of these observations is the presence of peaks near threshold in the mass spectra of the baryon-antibaryon pair. These enhancements are not likely to be resonance states, as the baryon angular distributions are not symmetric in their respective helicity frames [6]. Other visible structures in the mass spectra arise from charmonium decays. It is natural to compare the baryon angular distributions from charmonium decays with those in the region of the threshold enhancement. There is particular interest in $J/\psi \rightarrow p\bar{p}$, where the proton angular distribution has been studied by DASP [7], DM2 [10], Mark I [8], Mark II [9] and BES [11, 12, 13]. J/ψ mesons from the reaction $e^+e^- \rightarrow J/\psi$ are produced predominantly in helicity ± 1 states. Therefore, the baryon angular distributions are proportional to $1 + \alpha \cos^2 \theta$, where θ is the baryon polar angle in the J/ψ helicity frame. Many theoretical predictions [14] exist for the value of α .

Study of two-body baryonic decays of charmonia at a B -factory has several different features as compared with an e^+e^- machine running at the J/ψ mass. J/ψ mesons from the two body decay of B mesons accompanied by spin zero particles are in a pure helicity zero state. This provides a useful cross check for previous measurements. The charmonia from B decays do not suffer from poor acceptance near the beam pipe, and events with $|\cos \theta|$ near 1 can be detected. Such events are very effective for determining α . Requiring that the J/ψ originate from a B decay eliminates $e^+e^- \rightarrow q\bar{q} \rightarrow p\bar{p}$ background, where q stands for a u or d quark. For $e^+e^- \rightarrow J/\psi \rightarrow p\bar{p}$, this background cannot be separated from the signal on an event-by-event basis.

In the study of two-body baryonic decays of charmonia we focus on the decay processes $B^+ \rightarrow p\bar{p}K^+$ and $B^+ \rightarrow \Lambda\bar{\Lambda}K^+$ [15]. We report the first observation of $\eta_c \rightarrow \Lambda\bar{\Lambda}$. There is little information about η_c decays into baryon-antibaryon pairs except for $\eta_c \rightarrow p\bar{p}$. Measuring decay rates of the η_c to different baryon-antibaryon modes is a useful check for theoretical predictions [16] and can shed light on quark-diquark dynamics.

We use a 357 fb^{-1} data sample consisting of 386×10^6 $B\bar{B}$ pairs collected by the Belle detector at the KEKB asymmetric energy e^+e^- (3.5 on 8 GeV) collider [17]. The Belle detector is a large solid angle magnetic spectrometer that consists of a four layer silicon vertex detector (SVD), a 50 layer central drift chamber (CDC), an array of aerogel threshold Čerenkov counters (ACC), a barrel-like arrangement of time of flight scintillation counters (TOF), and an electromagnetic calorimeter comprised of CsI (Tl) crystals located inside a superconducting solenoid coil that provides a 1.5 T magnetic field. An iron flux return located outside of the coil is instrumented to detect K_L^0 mesons and to identify muons. The detector is described in detail elsewhere [18].

The event selection criteria are based on information obtained from the tracking system (SVD+CDC) and the hadron identification system (CDC+ACC+TOF). We follow the same procedure as in ref. [3] to select proton and kaon candidates. Λ candidates are reconstructed via the $p\pi^-$ channel using the method described in ref. [19].

To identify the reconstructed B meson candidates, we use the beam energy constrained mass $M_{bc} = \sqrt{E_{\text{beam}}^2 - p_B^2}$ and the energy difference $\Delta E = E_B - E_{\text{beam}}$, where E_{beam} is the beam energy, and p_B and E_B are the momentum and energy of the reconstructed B meson in the rest frame of the $\Upsilon(4S)$. The signal region is defined as $5.2 \text{ GeV}/c^2 < M_{bc} < 5.29 \text{ GeV}/c^2$ and $-0.1 \text{ GeV} < \Delta E < 0.2 \text{ GeV}$. The signal peaks at $M_{bc} = 5.279 \text{ GeV}/c^2$ and $\Delta E = 0$.

The dominant background arises from continuum $e^+e^- \rightarrow q\bar{q}$ processes. The background from $b \rightarrow c$ and from B decays into charmless final states is negligible. In the $\Upsilon(4S)$ rest frame, continuum events are jet-like while $B\bar{B}$ events are more spherical. The reconstructed

momenta of final state particles are used to form several event shape variables (e.g. thrust angle, Fox-Wolfram moments, etc.) in order to categorize each event. We follow the scheme described in ref. [20] that combines seven event shape variables into a Fisher discriminant to suppress continuum background.

Probability density functions (PDFs) for the Fisher discriminant and the cosine of the angle between the B flight direction and the beam direction in the $\Upsilon(4S)$ rest frame are combined to form the signal (background) likelihood $\mathcal{L}_{s(b)}$. The signal PDFs are determined from GEANT based Monte Carlo (MC) simulation and the background PDFs are obtained from sideband data with $M_{bc} < 5.26 \text{ GeV}/c^2$. We require the likelihood ratio $\mathcal{R} = \mathcal{L}_s/(\mathcal{L}_s + \mathcal{L}_b)$ to be greater than 0.4 for both $p\bar{p}K^+$ and $\Lambda\bar{\Lambda}K^+$ modes. These selection criteria suppress approximately 69% (66%) of the background while retaining 92% (91%) of the signal for the $p\bar{p}K^+$ ($\Lambda\bar{\Lambda}K^+$) mode. If there are multiple B candidates in an event, we select the one with the best χ^2 value from the B decay vertex fit. Multiple B candidates are found in less than 2% (5%) of events for the $p\bar{p}K^+$ ($\Lambda\bar{\Lambda}K^+$) mode.

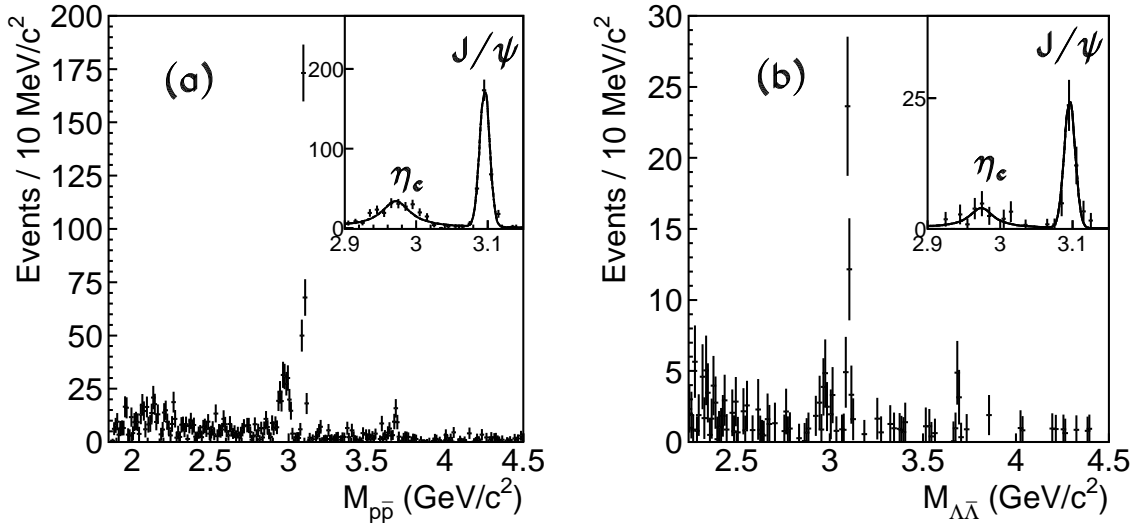


FIG. 1: (a) B signal yield versus $M_{p\bar{p}}$ and (b) B signal yield versus $M_{\Lambda\bar{\Lambda}}$. The inset shows the η_c - J/ψ mass region. The curves represent the unbinned likelihood fits to the data.

We use an unbinned extended maximum likelihood fit to estimate the B signal yield. For the signal PDF, we use a Gaussian in M_{bc} and a double Gaussian in ΔE . We fix the parameters of these functions to the values determined from MC simulation [21]. Background shapes are fixed from fitting to the sideband events in the region $3.14 \text{ GeV}/c^2 < M_{p\bar{p}} < 3.34 \text{ GeV}/c^2$. The M_{bc} background is modeled using a parametrization used by the ARGUS collaboration [22]. The ΔE background shape is modeled by a first order polynomial.

We determine B signal yields in 10 MeV/c² wide $M_{p\bar{p}}$ ($M_{\Lambda\bar{\Lambda}}$) mass bins from the kinematic threshold to 4.5 GeV/c²; the result is shown in Fig. 1(a) (Fig. 1(b)). There are clear η_c and J/ψ peaks in the mass spectrum. We use a relativistic Breit-Wigner function for the η_c peak, a Gaussian for the J/ψ peak, and a linear function for the non-resonant background. The Breit-Wigner function is convolved with the detector response function, which is taken from the J/ψ peak. A maximum likelihood fit to the data is shown in the inset. We obtain an η_c mass of $M_{\eta_c} = 2971 \pm 3_{-1}^{+2} \text{ MeV}/c^2$ ($2974 \pm 7_{-1}^{+2} \text{ MeV}/c^2$) and a width of $\Gamma(\eta_c) = 48_{-7}^{+8} \pm 5$

MeV/ c^2 ($40 \pm 19 \pm 5$ MeV/ c^2) for the $\eta_c \rightarrow p\bar{p}$ ($\eta_c \rightarrow \Lambda\bar{\Lambda}$) mode. The systematic errors are determined from the differences of J/ψ peaks between data and the PDG [25] value, and by varying different fit shapes for η_c signal and background assuming no interference effect between them. The width is larger than the PDG average but is consistent with recent BaBar [5, 23] and previous Belle [24] measurements.

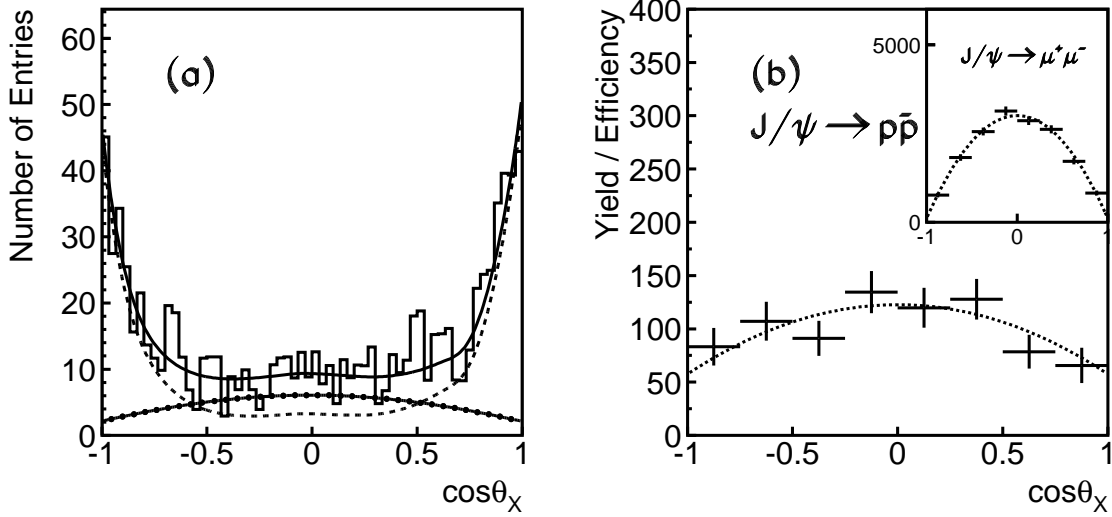


FIG. 2: (a) Likelihood fit and (b) χ^2 fit results of the $J/\psi \rightarrow p\bar{p}$ helicity angle distribution. In the maximum likelihood fit plot, the solid, dotted solid, and dashed line represent the combined fit result, fitted signal, and fitted background, respectively. In the χ^2 fit plot, the inset shows the fit result for B signal yield of $B^+ \rightarrow J/\psi K^+$, $J/\psi \rightarrow \mu^+\mu^-$.

We define the J/ψ signal region as $3.075 \text{ GeV}/c^2 < M_{p\bar{p}} < 3.117 \text{ GeV}/c^2$ and use events in this signal region to study the proton angular distribution in the helicity frame of the J/ψ . The helicity angle θ_X is defined as the angle between the proton flight direction and the direction opposite to the flight of the kaon in the J/ψ rest frame. The angular distribution of J/ψ in the helicity zero state is parameterized as $P(\alpha_B, \cos \theta_X) = (1 + \alpha_B \cos^2 \theta_X) / (2 + 2\alpha_B/3)$ with $\alpha_B = -2\alpha/(\alpha + 1)$ [26]. Here, α is the anisotropy parameter determined from the angular distribution of J/ψ in helicity $= \pm 1$ states produced in $e^+e^- \rightarrow J/\psi$. Previous measurements [7, 8, 9, 10, 11, 12, 13] give an average of $\alpha = 0.66 \pm 0.05$ for $p\bar{p}$ and $\alpha = 0.65 \pm 0.11$ for $\Lambda\bar{\Lambda}$; these values correspond to $\alpha_B = -0.80 \pm 0.04$ for $p\bar{p}$ and $\alpha_B = -0.79 \pm 0.08$ for $\Lambda\bar{\Lambda}$.

For analysis of the angular distribution, we define a likelihood L ,

$$\frac{e^{-(N_s+N_b)}}{N!} \prod_{i=1}^N [N_s P_s(M_{bc_i}, \Delta E_i) \epsilon(\cos \theta_{Xi}) P(\alpha_B, \cos \theta_{Xi}) + N_b P_b(M_{bc_i}, \Delta E_i, \cos \theta_{Xi})],$$

where α_B is a fit parameter in addition to N_s and N_b , $\epsilon(\cos \theta_X)$ is the efficiency function and ϵP is normalized to 1. The efficiency $\epsilon(\cos \theta_X)$ obtained from the signal MC simulation is flat as a function of $\cos \theta_X$. From a study of signal MC simulation, we find that there is no correlation between M_{bc} , ΔE and θ_X . The background PDF as a function of M_{bc} , ΔE , and

$\cos\theta_X$ is determined from $M_{p\bar{p}}$ sideband data. Fig. 2(a) shows the result of the fit to the $J/\psi \rightarrow p\bar{p}$ candidates in the entire M_{bc} , ΔE region. We determine α_B to be -0.60 ± 0.13 . As a cross-check, we use a χ^2 method and fit the efficiency corrected B signal yields in bins of $\cos\theta_X$ to a $1 + \alpha_B \cos^2\theta_X$ parametrization. The results of the fit are shown in Fig. 2(b). We obtain $\alpha_B = -0.53 \pm 0.15$ with $\chi^2/d.o.f. = 0.9$, consistent with the result of the unbinned fit. We measure the angular distribution of $J/\psi \rightarrow \mu^+\mu^-$ decays from $B^+ \rightarrow J/\psi K^+$ to verify the fitting procedure. The result is shown in the inset of Fig. 2(b). The fitted value agrees with the expectation for massless fermions.

We determine the systematic error in α_B by varying the value of various selection cuts and parameters of PDFs to check for trends in the value of α_B . These trends are parametrized by a linear function. We then quote the change in α_B along the line between the selected point and the far end of the tested region as a systematic error. Note that this is a conservative estimate, since statistical fluctuations also contribute to changes in α_B . We assign a systematic error of 0.08 for the \mathcal{R} selection, 0.06 for proton/kaon selection, and 0.02 for fitting PDFs. Other systematic errors are negligible. The observed difference between the maximum likelihood method and the χ^2 method is also included in the systematic error. The total systematic uncertainty in α_B is 0.13.

There are several complicating factors in the analysis of $B^+ \rightarrow \Lambda \bar{\Lambda} K^+$ decays relative to $B^+ \rightarrow p\bar{p}K^+$ decays. The efficiency for detecting slow pion from Λ decays is small. As a result, the Λ reconstruction efficiency is non-uniform as a function of polar angle ($\cos\theta_p$) of the secondary proton in the Λ helicity frame, and is correlated with $\cos\theta_X$, where X refers to the Λ . The likelihood function is similar to the previous one except that the angular part contains two more variables, $\cos\theta_p$ and $\cos\theta_{\bar{p}}$. The efficiency function $\epsilon(\cos\theta_X, \cos\theta_p, \cos\theta_{\bar{p}})$ is obtained from a signal MC sample with 4×10^6 events. The background PDF is determined from $M_{\Lambda\bar{\Lambda}}$ sideband data in the region $3.14 \text{ GeV}/c^2 < M_{\Lambda\bar{\Lambda}} < 3.54 \text{ GeV}/c^2$. The value of α_B obtained from the maximum likelihood fit is $-0.44 \pm 0.51 \pm 0.31$, where the systematic error is determined from the same procedure as that used for $J/\psi \rightarrow p\bar{p}$ decays.

We define an η_c signal region as $2.94 \text{ GeV}/c^2 < M_{\Lambda\bar{\Lambda}} < 3.02 \text{ GeV}/c^2$. Signal peaks are visible in the M_{bc} and ΔE distributions. The fitted B signal yield, efficiency, and obtained branching fraction are shown in Table I. The maximum likelihood fit for $B^+ \rightarrow \eta_c K^+$, $\eta_c \rightarrow \Lambda\bar{\Lambda}$ gives a yield of $19.5^{+5.1}_{-4.4}$ with a statistical significance of 7.9 standard deviations. The significance is defined as $\sqrt{-2\ln(L_0/L_{\max})}$, where L_0 and L_{\max} are the likelihood values returned by the fit with the signal yield fixed to zero and at its best fit value, respectively. The fit yield is consistent with the yield (18.2 ± 4.8) obtained from the first fit shown in Fig. 1(b). As a cross check, the obtained $\mathcal{B}(J/\psi \rightarrow p\bar{p}, \Lambda\bar{\Lambda})$ are in good agreement with the world average and with the latest BES result [13]. We also determine the branching fraction ratios: $\mathcal{B}(\eta_c \rightarrow \Lambda\bar{\Lambda})/\mathcal{B}(\eta_c \rightarrow p\bar{p}) = 0.67^{+0.19}_{-0.16} \pm 0.12$ and $\mathcal{B}(J/\psi \rightarrow \Lambda\bar{\Lambda})/\mathcal{B}(J/\psi \rightarrow p\bar{p}) = 0.90^{+0.15}_{-0.14} \pm 0.10$, where common systematic errors in the numerator and denominator cancel.

TABLE I: Measured branching fractions for $J/\psi, \eta_c \rightarrow p\bar{p}, \Lambda\bar{\Lambda}$

Modes	Yield	Eff.(%)	B.F.Product(10^{-6})	$\mathcal{B}(J/\psi, \eta_c \rightarrow p\bar{p}, \Lambda\bar{\Lambda})(10^{-3})$
$B^+ \rightarrow \eta_c K^+, \eta_c \rightarrow p\bar{p}$	195_{-15}^{+16}	$35.8_{-0.3}^{+0.3}$	$1.42_{-0.11}^{+0.11} {}_{-0.20}^{+0.16}$	$1.58 \pm 0.12 {}_{-0.22}^{+0.18} \pm 0.47^a$
$B^+ \rightarrow \eta_c K^+, \eta_c \rightarrow \Lambda\bar{\Lambda}$	$19.5_{-4.5}^{+5.2}$	$5.3_{-0.1}^{+0.1}$	$0.95_{-0.22}^{+0.25} {}_{-0.11}^{+0.08}$	$0.87_{-0.21}^{+0.24} {}_{-0.14}^{+0.09} \pm 0.27^b$
$B^+ \rightarrow J/\psi K^+, J/\psi \rightarrow p\bar{p}$	317_{-18}^{+19}	$37.3_{-0.4}^{+0.4}$	$2.21_{-0.13}^{+0.13} \pm 0.10$	$2.21 \pm 0.13 \pm 0.31 \pm 0.10^c$
$B^+ \rightarrow J/\psi K^+, J/\psi \rightarrow \Lambda\bar{\Lambda}$	$45.9_{-6.7}^{+7.7}$	$5.9_{-0.3}^{+0.3}$	$2.00_{-0.29}^{+0.34} \pm 0.34$	$2.00_{-0.29}^{+0.34} \pm 0.34 \pm 0.08^c$

^a $\mathcal{B}(B^+ \rightarrow \eta_c K^+) = 0.9 \pm 0.27 \times 10^{-3}$ [25].

^b We use $\mathcal{B}(B^+ \rightarrow \eta_c K^+, \eta_c \rightarrow \Lambda\bar{\Lambda})/\mathcal{B}(B^+ \rightarrow \eta_c K^+, \eta_c \rightarrow p\bar{p}) = 0.67_{-0.16}^{+0.19} \pm 0.12$ measured in this paper and $\mathcal{B}(\eta_c \rightarrow p\bar{p}) = 1.3 \pm 0.4 \times 10^{-3}$ [25].

^c $\mathcal{B}(B^+ \rightarrow J/\psi K^+) = 1.00 \pm 0.04 \times 10^{-3}$ [25].

Systematic uncertainties are studied using high statistics control samples. For proton identification, we use a $\Lambda \rightarrow p\pi^-$ sample, while for K/π identification we use a $D^{*+} \rightarrow D^0\pi^+$, $D^0 \rightarrow K^-\pi^+$ sample. The tracking efficiency is studied with fully and partially reconstructed D^* samples. The modeling of the \mathcal{R} continuum suppression requirement is studied with the a topologically similar control sample, $B^+ \rightarrow J/\psi K^+, J/\psi \rightarrow \mu^+\mu^-$. For Λ reconstruction, we have an additional uncertainty on the efficiency for detecting tracks away from the IP. The size of this uncertainty is determined from the difference between Λ decay-time distributions in data and MC simulation. Based on these studies, we assign a 1% error for each track, 2% for each proton identification, 1% for each kaon/pion identification, an additional 3% for Λ reconstruction and 3% for the \mathcal{R} selection.

The systematic uncertainty in the fit yield is studied by varying the parameters of the signal and background PDFs and is approximately 5%. The MC statistical uncertainty and modeling contributes a 5% error. The error on the number of $B\bar{B}$ pairs is determined to be 1%, where the branching fractions of $\Upsilon(4S)$ to neutral and charged $B\bar{B}$ pairs are assumed to be equal. The non-charmonium feed-down background below the η_c mass region is estimated to be 8% and 12% for the $p\bar{p}$ and $\Lambda\bar{\Lambda}$ modes, respectively.

The correlated errors are added linearly and combined quadratically with the uncorrelated errors in the systematic error calculation. The total systematic uncertainties are 14% and 17% for the $p\bar{p}K^+$, and $\Lambda\bar{\Lambda}K^+$ modes, respectively.

In summary, using 386×10^6 $B\bar{B}$ events, we measure the branching fractions of $J/\psi \rightarrow p\bar{p}$, $\eta_c \rightarrow p\bar{p}$, $J/\psi \rightarrow \Lambda\bar{\Lambda}$ and $\eta_c \rightarrow \Lambda\bar{\Lambda}$ from $B^+ \rightarrow p\bar{p}K^+$ and $B^+ \rightarrow \Lambda\bar{\Lambda}K^+$ decays. We measure the parameter α_B for baryonic J/ψ decays. The parameters α_B are $-0.60 \pm 0.13 \pm 0.14$ and $-0.44 \pm 0.51 \pm 0.31$ for $J/\psi \rightarrow p\bar{p}$ and $J/\psi \rightarrow \Lambda\bar{\Lambda}$, respectively. This gives an α value for $J/\psi \rightarrow p\bar{p}$ of $0.43 \pm 0.13 \pm 0.14$, which is smaller than, but still consistent with, the current world average 0.66 ± 0.05 . We also report the first observation of $\eta_c \rightarrow \Lambda\bar{\Lambda}$ decays with $\mathcal{B}(\eta_c \rightarrow \Lambda\bar{\Lambda}) = (0.87_{-0.21}^{+0.24} {}_{-0.14}^{+0.09} \pm 0.27) \times 10^{-3}$. The observed ratio $\mathcal{B}(\eta_c \rightarrow \Lambda\bar{\Lambda})/\mathcal{B}(\eta_c \rightarrow p\bar{p})$ is $0.67_{-0.16}^{+0.19} \pm 0.12$, which is consistent with theoretical expectation [16].

We thank the KEKB group for excellent operation of the accelerator, the KEK cryogenics group for efficient solenoid operations, and the KEK computer group and the NII for valuable computing and Super-SINET network support. We acknowledge support from MEXT and JSPS (Japan); ARC and DEST (Australia); NSFC and KIP of CAS (contract No. 10575109 and IHEP-U-503, China); DST (India); the BK21 program of MOEHRD, and the CHEP SRC and BR (grant No. R01-2005-000-10089-0) programs of KOSEF (Korea); KBN (contract No. 2P03B 01324, Poland); MIST (Russia); ARRS (Slovenia); SNSF (Switzerland); NSC and MOE (Taiwan); and DOE (USA).

-
- [1] K. Abe *et al.* (Belle Collaboration), Phys. Rev. Lett. **88**, 181803 (2002).
 - [2] M.Z. Wang, Y.J. Lee *et al.* (Belle Collaboration), Phys. Rev. Lett. **90**, 201802 (2003).
 - [3] M.Z. Wang *et al.* (Belle Collaboration), Phys. Rev. Lett. **92**, 131801 (2004).
 - [4] Y.J. Lee, M.Z. Wang *et al.* (Belle Collaboration), Phys. Rev. Lett. **93**, 211801 (2004).
 - [5] B. Aubert *et al.* (BaBar Collaboration), Phys. Rev. D **72**, 051101 (2005).
 - [6] M.Z. Wang *et al.* (Belle Collaboration), Phys. Lett. B **617**, 141 (2005).
 - [7] R. Brandelik *et al.*, Phys. C **1**, 233 (1976).
 - [8] I. Peruzzi *et al.*, Phys. Rev. D **17**, 2901 (1978).
 - [9] M.W. Eaton *et al.*, Phys. Rev. D **29**, 804 (1984).
 - [10] D. Pallin *et al.*, Nucl. Phys. B **292**, 653 (1987).
 - [11] J.Z. Bai *et al.*, (BES Collaboration), Phys. Lett. B **591**, 42(2004).
 - [12] J.Z. Bai *et al.* (BES Collaboration), Phys. Lett. B **424**, 213 (1998).
 - [13] M. Ablikim *et al.* (BES Collaboration), Phys. Lett. B **632**, 181 (2006).
 - [14] S.J. Brodsky, G.P. Lepage, Phys. Rev. D **24**, 2848 (1981); M. Claudson, S.L. Glashow, M.B. Wise, Phys. Rev. D **25**, 1345 (1982); C. Carimalo Int. J. Mod. Phys. A **2**, 249 (1987).
 - [15] Throughout this report, inclusion of charge conjugate mode is always implied unless otherwise stated.
 - [16] M. Anselmino, F. Caruso, S. Forte and B. Pire, Phys. Rev. D **38**, 3516 (1988).
 - [17] S. Kurokawa and E. Kikutani *et al.*, Nucl. Instr. and Meth. A **499**, 1 (2003).
 - [18] A. Abashian *et al.* (Belle Collaboration), Nucl. Instr. and Meth. A **479**, 117 (2002).
 - [19] K. Abe *et al.* (Belle Collaboration), Phys. Rev. D **65**, 091103 (2002).
 - [20] K. Abe *et al.* (Belle Collaboration), Phys. Lett. **B517**, 309 (2001).
 - [21] There are corrections (-2.3 MeV, 0.5 MeV in mean shift on $\Delta E, M_{bc}$ and $0.98, 1.14$ in width scale on $\Delta E, M_{bc}$ respectively) applied to these parameters based on the measured difference between data and MC simulation for $B \rightarrow D\pi$ decays.
 - [22] H. Albrecht *et al.* (ARGUS Collaboration), Phys. Lett. B **229**, 304 (1989).
 - [23] B. Aubert *et al.* (BaBar Collaboration), Phys. Rev. Lett. **92**, 142002 (2004).
 - [24] F. Fang *et al.* (Belle Collaboration), Phys. Rev. Lett. **90**, 071801 (2003).
 - [25] S. Eidelman *et al.* (Particle Data Group), Phys. Lett. B **592**, 1 (2004).
 - [26] F. Murgia and M. Melis, Phys. Rev. D **51**, 3487 (1995).